

Communication

# Frequency offset refocused PISEMA-type sequences

Sergey V. Dvinskikh <sup>\*,1</sup>, Dick Sandström

*Division of Physical Chemistry, Arrhenius Laboratory, Stockholm University, SE-10691 Stockholm, Sweden*

Received 1 February 2005; revised 15 March 2005

Available online 22 April 2005

## Abstract

The popular PISEMA experiment is highly sensitive to the  $^1\text{H}$  chemical shift dispersion and the choice of the  $^1\text{H}$  carrier frequency. This is due to the off-resonance  $^1\text{H}$  irradiation in the FSLG-CP sequence employed during the dipolar evolution period. In the modified approach described in this work, the interfering frequency offset terms are suppressed. In the new pulse schemes, conventional FSLG-CP is intercalated with  $180^\circ$  pulses applied simultaneously to both frequency channels, and with phases set orthogonal to those of the spin-lock fields. The technique is demonstrated on a nematic liquid-crystalline sample. Extensions to amplitude-modulated FSLG-CP recoupling under MAS are also presented.

© 2005 Elsevier Inc. All rights reserved.

*Keywords:* Separated local field spectroscopy; Dipolar couplings; MAS; PISEMA; Cross-polarization

## 1. Introduction

Two-dimensional (2D) separated local field (SLF) spectroscopy [1] is a powerful NMR technique to measure and assign heteronuclear dipolar couplings between abundant and rare spins. Over the years, several advanced SLF pulse sequences have been developed which yield simple spectra with high dipolar resolution [2,3]. In particular, the polarization inversion spin exchange at the magic angle (PISEMA) experiment [4] is a well-established approach for NMR studies of macroscopically oriented samples such as biomolecules in membranes [3,5] and thermotropic liquid crystals [6–9]. The method is based on cross-polarization (CP) combined with flip-flop frequency- and phase-switched Lee–Goldburg (FSLG) homonuclear decoupling [10]. Compared to other competing techniques [1,2], PISEMA has a high dipolar scaling factor, a short radiofrequency (RF) cycle time, and efficiently suppresses perturbing  $^1\text{H}$ – $^1\text{H}$  dipolar

interactions at low RF power levels. These features facilitate accurate measurements of heteronuclear dipolar couplings over a wide range of magnitudes in anisotropic liquids and solids.

There is, however, a serious problem associated with FSLG-CP (i.e., the RF pulses applied during the evolution period in the PISEMA experiment)—the sequence is very sensitive to the  $^1\text{H}$  chemical shift and frequency offset. These parameters affect the dipolar splitting and resolution, and may reduce the signal intensity [7,11,12]. Smaller coupling are more susceptible to such effects. This shortcoming limits the application of the technique in systems which exhibit large  $^1\text{H}$  chemical shift dispersions and dipolar couplings heavily attenuated by molecular motions. Recently, this problem was approached by employing an on-resonance magic-echo-type sequence instead of off-resonance FSLG [12]. Although the on-resonance technique results in a reduced  $^1\text{H}$  offset dependence, the experimental dipolar linewidths are broader and the scaling factor is smaller as compared to those obtained by PISEMA under optimal conditions [12]. Herein, we describe an alternative approach to deal with offset effects in PISEMA which preserves all advantages of the original technique.

\* Corresponding author. Fax: +46 8 15 21 87.

E-mail address: [sergey@phycs.su.se](mailto:sergey@phycs.su.se) (S.V. Dvinskikh).

<sup>1</sup> On leave from the Institute of Physics, St. Petersburg State University, 198504 St. Petersburg, Russia.

Briefly, the frequency offset is refocused by repetitive  $180^\circ$  pulses inserted in the conventional FSLG-CP scheme. The performance of the new technique is studied by numerical simulations, and by experiments on a macroscopically oriented liquid-crystalline sample. Preliminary experiments on powdered solids carried out under magic-angle spinning (MAS) are also presented.

## 2. Pulse sequences

The conventional 2D PISEMA pulse sequence [4] is shown in Fig. 1A. After standard  $^1\text{H}$ – $^{13}\text{C}$  ramped-CP [13], the  $^1\text{H}$  magnetization is aligned at the magic angle with respect to the static magnetic field by means of a  $^1\text{H}$   $35^\circ$  pulse. It is subsequently spin-locked by off-resonance FSLG irradiation and matched by a phase-alternated  $^{13}\text{C}$  RF field at the Hartmann–Hahn (HH) condition  $\omega_{\text{eff,H}} - \omega_{1,\text{C}} = 0$ , where  $\omega_{\text{eff,H}} = (3/2)^{1/2} \gamma_{\text{H}} B_{1,\text{H}}$  and  $\omega_{1,\text{C}} = \gamma_{\text{C}} B_{1,\text{C}}$ . The dipolar evolution is initiated by phase inversion of the  $^1\text{H}$  spin-lock field with respect to the preparatory CP step. The heteronuclear dipolar couplings are monitored through the oscillations resulting from the coherent polarization transfer between  $^1\text{H}$  and  $^{13}\text{C}$  spins during  $t_1$ . The dipolar scaling factor of the sequence, when applied to static samples, is  $s^{\text{static}} = \sin \vartheta_m \approx 0.816$ , where  $\vartheta_m = 54.7^\circ$  is the magic angle.

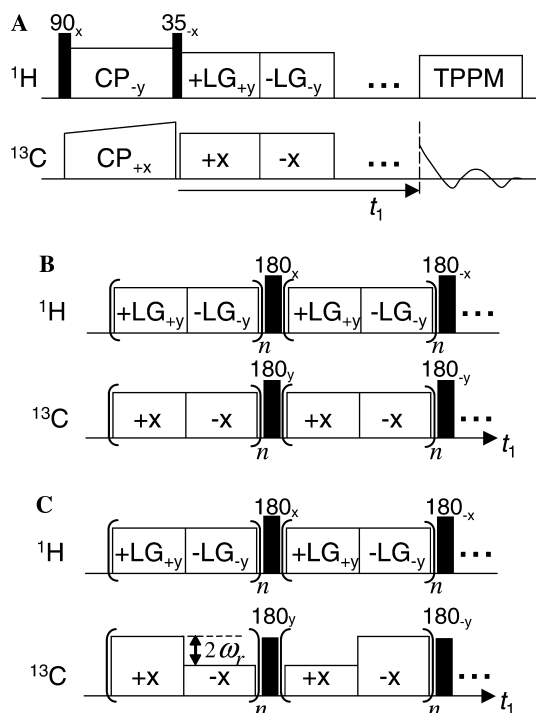


Fig. 1. (A) Conventional PISEMA [4] under stationary conditions employing FSLG-CP during the evolution period. (B) Frequency offset refocused FSLG-CP. (C) Frequency offset refocused FSLG-CP using amplitude modulation for heteronuclear dipolar recoupling under MAS.

In standard PISEMA, the  $^1\text{H}$  chemical shift  $\Delta\omega_I$  contributes with a term  $\cos(\vartheta_m)\Delta\omega_I I_z$  to the interaction frame Hamiltonian, and leads to an increase of the splitting  $\Delta\nu$  in the dipolar spectra [11]

$$2\pi\Delta\nu = 2\{[\sin(\vartheta_m)d_{IS}]^2 + [\cos(\vartheta_m)\Delta\omega_I]^2\}^{1/2}. \quad (1)$$

In the modified PISEMA sequence,  $180^\circ$  on-resonance pulses are inserted between series of  $n$  FSLG-CP blocks as shown in Fig. 1B. The directions of the RF fields during the refocusing pulses are, in rotating frame, orthogonal to the spin-lock fields. When applied simultaneously to both frequency channels, the  $180^\circ$  pulses preserve the heteronuclear dipolar evolution while frequency offset terms are suppressed.

For infinitely short  $180^\circ$  pulses, the relevant interaction frame Hamiltonians for two FSLG-CP periods separated by the refocusing pulses are given by

$$\tilde{H}_{(1)}^T = \sin(\vartheta_m)d_{IS}ZQ_x + \cos(\vartheta_m)\Delta\omega_I ZQ_z, \quad (2a)$$

$$\tilde{H}_{(2)}^T = \sin(\vartheta_m)d_{IS}ZQ_x - \cos(\vartheta_m)\Delta\omega_I ZQ_z, \quad (2b)$$

where  $ZQ_x$  are the single transition operators in the zero-quantum ( $ZQ$ ) subspace [14]. Written in this form, the offset contribution is analogous to the HH mismatch effect analyzed in [15]. In successive intervals, the precession axis in the  $ZQ$  subspace jumps between two directions given by the vectors  $(\sin(\vartheta_m)d_{IS}, 0, \pm \cos(\vartheta_m)\Delta\omega_I)$ . Efficient offset suppression is obtained when the delay between the jumps is short compared to the precession period [15]. Hence, refocusing must be performed fast on the time scale of the dipolar couplings and  $^1\text{H}$  chemical shifts.

The available sampling rate in  $t_1$  is, as in the conventional sequence, determined by the length of the FSLG block, and the receiver phase is cycled to account for the magnetization inversion by the  $180^\circ$  pulses. With infinitely short refocusing pulses, the scaling factor is the same as for the conventional sequence in Fig. 1A.

The extension of the new scheme to experiments carried out under fast MAS is shown in Fig. 1C. In this case, the  $^{13}\text{C}$  RF amplitude is modulated synchronously with the phase inversion to reintroduce the heteronuclear dipolar coupling under MAS as described in [16,17]. The dipolar scaling factor of this sequence is reduced to  $s^{\text{MAS}} = \cos \vartheta_m \approx 0.577$  due to sample spinning [17].

## 3. Numerical simulations

Numerically simulated spectra of isolated  $^1\text{H}$ – $^{13}\text{C}$  spin pairs under static conditions are shown in Fig. 2A assuming dipolar couplings of  $d_{\text{CH}}/2\pi = 5$  kHz (left column) and  $d_{\text{CH}}/2\pi = 2$  kHz (right column), respectively. The dipolar spectra in the top row were calculated for conventional PISEMA, and used a mean frequency of

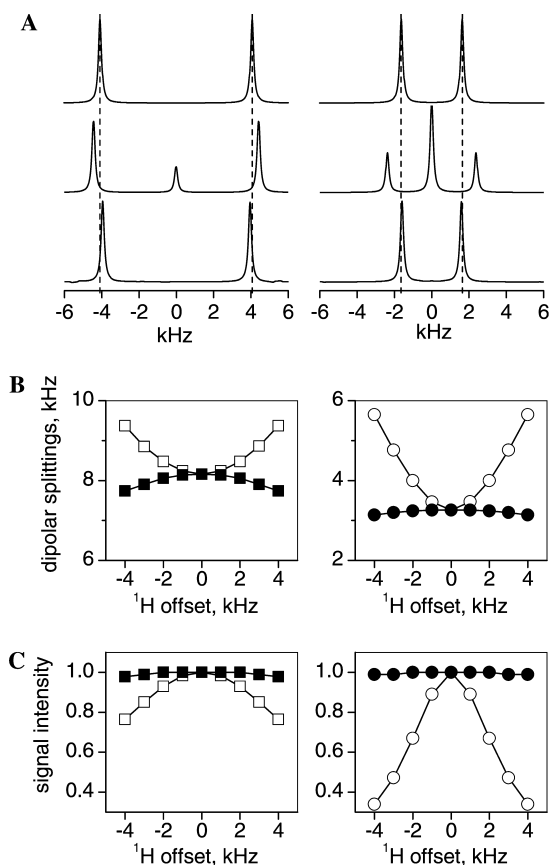


Fig. 2. (A) Simulated dipolar spectra for  $^1\text{H}$ - $^{13}\text{C}$  spin pairs with dipolar couplings  $d_{\text{CH}}/2\pi = 5$  and 2 kHz (left and right columns, respectively), and with a mean  $^1\text{H}$  frequency of 0 (top row) and 3 kHz (middle and bottom rows) during FSLG irradiation. The top and middle spectra were obtained by conventional PISEMA (cf. Fig. 1A), while the frequency offset refocused sequence in Fig. 1B was used to simulate the bottom spectra. The  $^1\text{H}$  RF field strength was 50 kHz. In the modified sequence,  $5.0 \mu\text{s}$  refocusing  $180^\circ$  pulses were inserted after  $n = 2$  FSLG-CP blocks. Panels (B) and (C) show offset dependences of, respectively, dipolar splittings and doublet peak intensities simulated for conventional (open symbols) and modified PISEMA (filled symbols). Results for  $^1\text{H}$ - $^{13}\text{C}$  spin pairs with  $d_{\text{CH}}/2\pi = 5$  kHz (left panel) and 2 kHz (right panel) are shown. The dipolar splittings produced by the modified sequence have been scaled with a factor of (1–0.035) to account for the finite width of the refocusing pulses.

the  $^1\text{H}$  FSLG irradiation corresponding to zero resonance offset. The spectral splittings are in this case given by  $2\pi\Delta\nu = 2\sin(\vartheta_m)d_{\text{CH}}$ . In the presence of a 3 kHz shift of the mean  $^1\text{H}$  frequency, the splittings increase and the doublet intensities decrease (see Fig. 2A, middle row). The effect is stronger for smaller couplings.

Spectra obtained by the modified sequence (with  $n = 2$ , cf. Fig. 1B) and at a 3 kHz shift of the mean  $^1\text{H}$  frequency are shown in the bottom row of Fig. 2A (spectra at zero shift coincide with the spectra in the top row). Clearly, the offset effect is suppressed in this case.

In Figs. 2B and C, simulated dipolar splittings and doublet intensities, respectively, are plotted as functions of the mean  $^1\text{H}$  frequency shift. In conventional

PISEMA, the splittings significantly increase and the intensities decrease with frequency shifts in either direction from the optimal value. The effect is, again, stronger for smaller couplings. For the modified method, in contrast, these effects are highly suppressed.

## 4. Experimental results

### 4.1. Oriented liquid crystal under static conditions

The performance of the frequency offset refocused PISEMA scheme was experimentally demonstrated on a static sample of 4-*n*-pentyl-4'-cyanobiphenyl (5CB) in the nematic phase, which orients spontaneously along the magnetic field of the spectrometer. Previously, conventional PISEMA spectra of 5CB have been reported in [7]. Due to the wide range of  $^1\text{H}$  chemical shifts in this sample, it was not possible to obtain optimally resolved and undistorted dipolar spectra for all chemical sites in a single 2D experiment. Rather, two separate experiments had to be performed in which the  $^1\text{H}$  offset was optimized for either the aliphatic or aromatic signals [7].

In contrast, very high resolution for all  $^{13}\text{C}$  sites is obtained in a single 2D experiment using the offset refocused PISEMA method (see Fig. 3A).  $180^\circ$  pulses with duration of  $5.3 \mu\text{s}$  were inserted after every other FSLG-CP block. Empirically, we found that  $n = 2$  results in adequate suppression of the offset effect for all  $^{13}\text{C}$  sites in this sample. The dipolar cross-sections in Fig. 3A for all resolved  $^{13}\text{C}$  peaks are very similar to those shown in [7]. In fact, some slices appear to be better resolved and less distorted, as compared to the previous results.

Fig. 3B compares the  $^1\text{H}$  shift dependence of  $^1\text{H}$ - $^{13}\text{C}$  dipolar splittings for selected aliphatic (top panel) and aromatic (bottom panel) sites in 5CB obtained by the conventional and modified PISEMA sequences. Using the conventional technique, a strong offset effect is observed. Optimal  $^1\text{H}$  offsets correspond to minimum splittings (indicated by dashed lines), and differ by more than 2 kHz for the aliphatic and aromatic sites. This value corresponds to the chemical shift difference of the aromatic and aliphatic protons at our magnetic field. Using the new sequence, the frequency offset effect is dramatically suppressed, especially for the aromatic sites which exhibit rather small dipolar splittings. Overall, the experimental observations are very similar to the simulation results in Fig. 2B.

### 4.2. Powder sample under MAS

Previously, an amplitude-modulated FSLG-CP scheme designed for efficient heteronuclear  $^1\text{H}$ - $^{13}\text{C}$  dipolar recoupling was described in [16,17]. Here, the

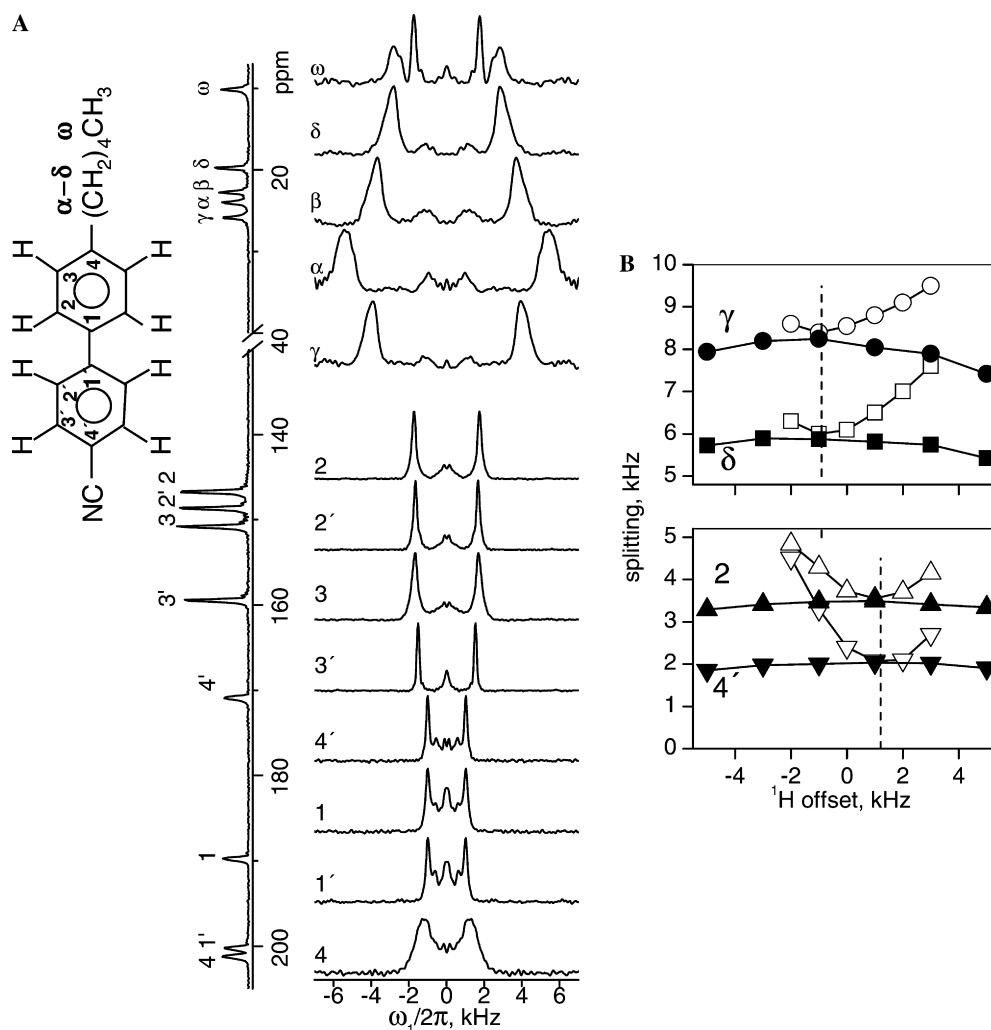


Fig. 3. (A)  $^1\text{H}$ - $^{13}\text{C}$  dipolar cross-sections through a 2D SLF spectrum of 5CB in nematic phase at 20 °C obtained by the offset refocused FSLG-CP sequence in Fig. 1B. The mean  $^1\text{H}$  frequency was set approximately to the centre of the  $^1\text{H}$  spectrum.  $180^\circ$  pulses of duration 5.3  $\mu\text{s}$  were inserted after every other FSLG-CP block (i.e.,  $n = 2$ , cf. Fig. 1B), and data sampling were performed after the  $180^\circ$  pulses. Four transients with a recycle delay of 10 s were accumulated for each of the 80  $t_1$  increments, which resulted in a total acquisition time of 53 min. The 1D  $^{13}\text{C}$  spectrum is shown to the left. (B) Experimental dipolar splittings of selected aliphatic,  $\gamma$  (circles) and  $\delta$  (squares), and aromatic, 2 (up-triangles) and 4' (down-triangles), sites as a function of the shift of the mean  $^1\text{H}$  frequency during FSLG irradiation. Open and filled symbols correspond to spectra obtained by conventional and modified PISEMA, respectively. Dashed lines indicate the optimal  $^1\text{H}$  frequency shift for aliphatic (top panel) and aromatic (bottom panel) sites.

performance of this sequence is compared to the offset refocused version shown in Fig. 1C. In Fig. 4A, we show dipolar spectra of  $[2\text{-}^{13}\text{C}, ^{15}\text{N}]\text{-L-alanine}$  obtained by the original and new sequences. The spectral shapes produced by the two techniques are very similar, and closely match the simulated powder spectrum (shown by a dashed line). The splittings between the outer singularities correspond to a  $^1\text{H}$ - $^{13}\text{C}$  dipolar coupling of 21 kHz, which is typical for  $\text{sp}^3$ -hybridized carbons in rigid systems [16,18].

In Fig. 4B, the  $^1\text{H}$  offset dependences of the spectral splittings are compared for the two methods. The strong offset effect observed when the original MAS technique is employed, is suppressed when the refocusing sequence is used.

## 5. Discussion and conclusions

The broadband performance of PISEMA sequences with respect to the choice of the  $^1\text{H}$  frequency is significantly improved by applying  $180^\circ$  pulses intercalating the FSLG-CP scheme. The overall effect is that heteronuclear dipolar splittings, linewidths, and signal intensities become much less susceptible to frequency offsets. This allows for accurate measurements of dipolar couplings in samples containing protons with distinctly different chemical shifts. Thus, the modified technique eliminates the necessity of performing separate SLF experiments with the  $^1\text{H}$  offset optimized for the best dipolar resolution for spins in different chemical environments, e.g., for aromatic and aliphatic sites in

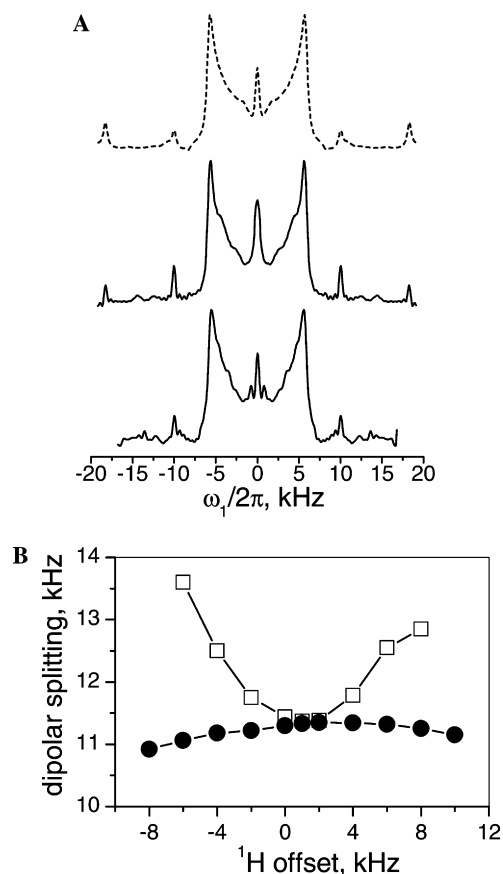


Fig. 4. (A)  $^1\text{H}$ – $^{13}\text{C}$  recoupled dipolar spectra of  $[2\text{-}^{13}\text{C}, ^{15}\text{N}]\text{-L-alanine}$  obtained at a spinning frequency of 10 kHz using the original FSLG-CP sequence [16] (middle spectrum), and the modified sequence in Fig. 1C (bottom spectrum). The  $^1\text{H}$  offsets are set close to the optimal value. In the modified sequence,  $180^\circ$  pulses of duration  $3.6\ \mu\text{s}$  were inserted after each FSLG-CP block (i.e.,  $n=1$ , cf. Fig. 1C). A numerically simulated spectrum for a  $^1\text{H}$ – $^{13}\text{C}$  spin pair assuming a dipolar coupling of  $d_{\text{CH}}/2\pi = 21\ \text{kHz}$  is shown at the top. (B) Experimental dipolar splittings (taken as distances between the outer singularities in the powder spectra) as a function of the shift of the mean  $^1\text{H}$  frequency during FSLG irradiation. Open and filled symbols correspond to spectra obtained by the original and modified FSLG-CP sequences, respectively.

thermotropic liquid crystals. Other important spin systems include the headgroup, glycerol backbone, and fatty acyl chains in lipid membranes [19,20]. Offset suppression is most important at high static magnetic fields.

The  $^{13}\text{C}$  frequency offset performance should, in principle, also be improved by the modified sequences. This is, however, of less concern since the  $^{13}\text{C}$  offset terms are already efficiently suppressed by the virtually in-transverse-plane spin-lock in the  $^{13}\text{C}$  channel.

We also verified by numerical simulations that the offset suppression effect is virtually the same for ideal and finite-duration  $180^\circ$  pulses, as long as the condition  $\tau_{180} \ll (n \times \tau)$  holds, where  $\tau$  is the length of the FSLG cycle. Refocusing pulses of finite duration, however, change the scaling factor of the sequence. The correction of the scaling factor is obtained by calculating the lowest

order interaction frame average dipolar Hamiltonian for an RF cycle consisting of two blocks of  $180^\circ$  pulse pairs and two FSLG-CP periods:

$$180^\circ_y(I, S) - (\text{FSLG-CP})_n - 180^\circ_y(I, S) - (\text{FSLG-CP})_n.$$

The interaction frame Hamiltonians during the four intervals,  $0 < t \leq \tau_{180}$ ,  $\tau_{180} < t \leq \tau_{180} + n\tau$ ,  $\tau_{180} + n\tau < t \leq 2\tau_{180} + n\tau$ , and  $2\tau_{180} + n\tau < t \leq 2\tau_{180} + 2n\tau$ , are given, respectively, by

$$\tilde{H}_{IS(1)}^T(t) = \sin(\vartheta_m) \cos^2(\omega_{180}t) d_{IS} Z Q_x, \quad (3a)$$

$$\tilde{H}_{IS(2)}^T = \sin(\vartheta_m) d_{IS} Z Q_x, \quad (3b)$$

$$\tilde{H}_{IS(3)}^T(t) = \sin(\vartheta_m) \cos^2[\omega_{180}(t - n\tau)] d_{IS} Z Q_x, \quad (3c)$$

$$\tilde{H}_{IS(4)}^T = \sin(\vartheta_m) d_{IS} Z Q_x. \quad (3d)$$

In this calculation, exact Hartmann–Hahn matching and zero chemical shifts were assumed. The average Hamiltonian for the cycle time  $\tau_c = 2n\tau + 2\tau_{180}$  is calculated to

$$\overline{\tilde{H}}_{IS}^T(\tau_c) = \sin(\vartheta_m) \left(1 - \frac{\tau_{180}}{\tau_c}\right) d_{IS} Z Q_x. \quad (4)$$

Thus, the conventional scaling factor  $\sin(\vartheta_m)$  is corrected by the coefficient  $(1 - \tau_{180}/\tau_c)$  due to the finite width of the refocusing pulses. With the experimental parameters used in this study, the scaling factor changes by less than 4 and 6%, for static and spinning samples, respectively. Importantly, the offset dependence of the scaling factor is flat over a wide range, which is in contrast to the situation for the conventional sequence.

Homonuclear  $^1\text{H}$ – $^1\text{H}$  couplings in anisotropic media are by no means negligible. For instance, the width of the  $^1\text{H}$  spectrum of 5CB in the nematic phase is around 20 kHz [21]. Experimental and simulation results indicate no deterioration of the homonuclear decoupling efficiency upon incorporation of the refocusing pulses into the FSLG sequence. Numerical simulations of  $^{13}\text{C}$ – $^1\text{H}_3$  spin systems including the homonuclear interactions reveal that the decoupling efficiencies of conventional and offset refocused FSLG are virtually identical, and that they are superior to continuous-wave LG irradiation (not shown).

Phase alternation of the refocusing pulses,  $180_{+y} - 180_{-y}$ , reduces RF field inhomogeneity effects. This approach, however, introduces an  $I_x$  offset term, which can be suppressed by a longer cycle,  $180_{+y} - 180_{-y} - 180_{-y} - 180_{+y}$ , or by further extensions according to MLEV schemes [22].

As demonstrated by the experimental results on powdered alanine, the offset refocused technique is also efficient when implemented under rapid sample spinning. However, the  $180^\circ$  pulses may complicate the spin dynamics under MAS due to interference with the sample

rotation, and may induce unwanted CSA and dipolar recoupling [23]. While such effects were not observed in the present experiments, it may occur at other combinations of the spinning speed and RF cycle time. In this work, the ratio between the RF cycle time and spinning frequency was chosen rather arbitrary, since the FSLG-CP sequence does not require rotor synchronization [17].

To summarize, the high sensitivity to the  $^1\text{H}$  frequency offset and chemical shift terms, characteristic of conventional PISEMA spectroscopy, is to a large extent suppressed in the modified NMR sequences introduced in this work. As a result, the resolution and accuracy of the extracted dipolar couplings are improved, and the requirement of a carefully chosen  $^1\text{H}$  carrier frequency is relaxed. The novel schemes were demonstrated on a liquid-crystalline sample under stationary conditions, and on a rigid solid under MAS. The approach is particularly useful for samples exhibiting small dipolar couplings and significant  $^1\text{H}$  chemical shift dispersion at high static magnetic field strengths.

## 6. Experimental

Unlabeled 5CB and [2- $^{13}\text{C}$ ,  $^{15}\text{N}$ ]-labeled L-alanine were purchased from Merck and Cambridge Isotope Laboratories, respectively, and used without further purification.

All NMR experiments were performed at a magnetic field of 9.4 T on a Chemagnetics Infinity-400 spectrometer. For the 5CB experiments, a 6 mm double-resonance MAS probe was used in the static mode. Ramped CP [13], with a nutation frequency of about 37 kHz and a contact time of 4 ms, was employed to prepare spin-locked magnetizations. Radiofrequency field strengths during  $t_1$  were 50 and 61 kHz in the  $^1\text{H}$  and  $^{13}\text{C}$  channels, respectively. Heteronuclear decoupling during the detection period was achieved by 30 kHz  $^1\text{H}$  TPPM irradiation [24]. Sample heating due to RF irradiation was  $<2^\circ\text{C}$  [7].

For the MAS experiments of the alanine sample, a 4 mm double-resonance MAS probe was used. Ramped CP, with a nutation frequency of about 60 kHz and a 0.6 ms contact time, was employed to prepare spin-locked magnetizations. A  $^1\text{H}$  RF field of 62.5 kHz was used during FSLG-CP. Heteronuclear decoupling was achieved by 80 kHz  $^1\text{H}$  TPPM irradiation.

Numerical simulations were performed using the SIMPSON programming package [25].

## Acknowledgments

This work was supported by the Swedish Research Council, the Carl Trygger Foundation, the Magn. Bergvall Foundation, and the Foundation of Lars Hierta's Memory.

## References

- [1] R.K. Hester, J.L. Ackerman, B.L. Neff, J.S. Waugh, Separated local field spectra in NMR: determination of structure of solids, *Phys. Rev. Lett.* 36 (1976) 1081–1083.
- [2] S. Caldarelli, Local field experiments in liquid crystals, in: D.M. Grant, R.K. Harris (Eds.), *Encyclopedia of Nuclear Magnetic Resonance*, Wiley, Chichester, 2002, pp. 291–298.
- [3] S.J. Opella, Multiple-resonance multi-dimensional solid-state NMR of proteins, in: D.M. Grant, R.K. Harris (Eds.), *Encyclopedia of Nuclear Magnetic Resonance*, Wiley, Chichester, 2002, pp. 427–436.
- [4] C.H. Wu, A. Ramamoorthy, S.J. Opella, High-resolution heteronuclear dipolar solid-state NMR spectroscopy, *J. Magn. Reson. Ser. A* 109 (1994) 270–272.
- [5] A. Ramamoorthy, Y. Wei, D.-K. Lee, PISEMA solid-state NMR spectroscopy, *Annu. Rep. NMR Spectrosc.* 52 (2004) 1–52.
- [6] S.V. Dvinskikh, Z. Luz, H. Zimmermann, A. Maliniak, D. Sandström, Molecular characterization of hexaoctyloxy-rufigallol in the solid and columnar phases: a local field NMR study, *J. Phys. Chem. B* 107 (2003) 1969–1976.
- [7] S.V. Dvinskikh, H. Zimmermann, A. Maliniak, D. Sandström, Separated local field spectroscopy of columnar and nematic liquid crystals, *J. Magn. Reson.* 163 (2003) 46–55.
- [8] D.-K. Lee, T. Narasimhaswamy, A. Ramamoorthy, PITAN-SEMA, a low-power PISEMA solid-state NMR experiment, *Chem. Phys. Lett.* 399 (2004) 359–362.
- [9] K. Nishimura, A. Naito, Dramatic reduction of the RF power for attenuation of sample heating in 2D-separated local field solid-state NMR spectroscopy, *Chem. Phys. Lett.* 402 (2005) 245–250.
- [10] A. Bielecki, A.C. Kolbert, H.J.M. de Groot, R.G. Griffin, M.H. Levitt, Frequency-switched Lee–Goldburg sequences in solids, *Adv. Magn. Reson.* 14 (1990) 111–124.
- [11] Z. Gan, Spin dynamics of polarization inversion spin exchange at the magic angle in multiple spin systems, *J. Magn. Reson.* 143 (2000) 136–143.
- [12] A.A. Nevzorov, S.J. Opella, A “Magic Sandwich” pulse sequence with reduced offset dependence for high-resolution separated local field spectroscopy, *J. Magn. Reson.* 164 (2003) 182–186.
- [13] G. Metz, X. Wu, S.O. Smith, Ramped-amplitude cross polarization in magic-angle-spinning NMR, *J. Magn. Reson. Ser. A* 110 (1994) 219–227.
- [14] M.H. Levitt, D. Suter, R.R. Ernst, Spin dynamics and thermodynamics in solid-state NMR cross polarization, *J. Chem. Phys.* 84 (1986) 4243–4255.
- [15] R. Fu, C. Tian, H. Kim, S.A. Smith, T.A. Cross, The effect of Hartmann–Hahn mismatching on polarization inversion spin exchange at the magic angle, *J. Magn. Reson.* 159 (2002) 167–174.
- [16] S.V. Dvinskikh, H. Zimmermann, A. Maliniak, D. Sandström, Heteronuclear dipolar recoupling in liquid crystals and solids by PISEMA-type pulse sequences, *J. Magn. Reson.* 164 (2003) 165–170.
- [17] S.V. Dvinskikh, H. Zimmermann, A. Maliniak, D. Sandström, Heteronuclear dipolar recoupling in solid-state nuclear magnetic resonance by amplitude-, phase-, and frequency-modulated Lee–Goldburg cross-polarization, *J. Chem. Phys.* 122 (2005) 044512.
- [18] S.V. Dvinskikh, H. Zimmermann, A. Maliniak, D. Sandström, Measurements of motionally-averaged heteronuclear dipolar couplings in MAS NMR using R-type recoupling, *J. Magn. Reson.* 168 (2004) 194–201.
- [19] S.V. Dvinskikh, V. Castro, D. Sandström, Heating caused by radiofrequency irradiation and sample rotation in  $^{13}\text{C}$  magic angle spinning NMR studies of lipid membranes, *Magn. Reson. Chem.* 42 (2004) 875–881.
- [20] S.V. Dvinskikh, V. Castro, D. Sandström, Efficient solid-state NMR methods for measuring heteronuclear dipolar couplings in

- unoriented lipid membrane systems, *Phys. Chem. Chem. Phys.* 7 (2005) 607–613.
- [21] S.V. Dvinskikh, I. Furó, Anisotropic self-diffusion in the nematic phase of a thermotropic liquid crystal by  $^1\text{H}$ -spin-echo nuclear magnetic resonance, *J. Chem. Phys.* 115 (2001) 1946–1950.
- [22] A.J. Shaka, Decoupling methods, in: D.M. Grant, R.K. Harris (Eds.), *Encyclopedia of Nuclear Magnetic Resonance*, Wiley, New York, 1996, pp. 1558–1564.
- [23] S. Dusold, A. Sebald, Dipolar recoupling under magic-angle spinning conditions, *Annu. Rep. NMR Spectrosc.* 41 (2000) 185–264.
- [24] A.E. Bennett, C.M. Rienstra, M. Auger, K.V. Lakshmi, R.G. Griffin, Heteronuclear decoupling in rotating solids, *J. Chem. Phys.* 103 (1995) 6951–6958.
- [25] M. Bak, J.T. Rasmussen, N.C. Nielsen, SIMPSON: A general simulation program for solid-state NMR spectroscopy, *J. Magn. Reson.* 147 (2000) 296–330.